Modelling the Heat Dissipation of a Head Lamp within COMSOL Multiphysics®

F. Viry[1], P. Namy[1], C. Dupuis[2]

1. SIMTEC, Grenoble, France.
2. Decathlon B'twin Village, Lille, France.

Abstract

In order to reduce the environmental footprint of a serial production of head lamps, one lever is to replace and employ new materials, often requiring to redesign the product to ensure its mechanical and thermal resistance. In this context, this paper studies the modelling of the heat dissipation of a head lamp within COMSOL Multiphysics®. The electronic components of the lamp produce heat by Joule effect, modelled as thermal sources. Within the lamp, the three heat transfer modes are modelled. The heat conduction is modelled in volumes using the Heat Transfer in Solids physics, and shell elements for thin volumes (*e.g.* the copper layout). Natural convection is modelled using the Nonisothermal Laminar Flow interface. The radiative transfers are taken into account using the Surface-to-surface Radiation physics. The heat transfers of the lamp with the surrounding environment are modelled using heat transfer coefficients for natural convection and radiative losses. To validate the model, experimental results are available on an existing lamp. When the lamp is open, temperature distributions are available thanks to thermal camera measurements, allowing a qualitative validation of the model. The model is then validated quantitatively in the closed lamp configuration using temperature measurements available thanks to thermocouples placed within the lamp. The model can then be used as a digital twin to assess the heat dissipation performance of new designs by forecasting the temperature field and the hot spots within the lamp.

Keywords: heat dissipation, heat conduction, natural convection, radiative transfers, shell elements, heat transfer.

1 Introduction

In order to reduce the environmental footprint of a serial production of head lamps, one lever is to replace and employ new materials, often requiring to redesign the product to ensure its mechanical and thermal resistance. To assess the thermal performance of future designs of a head lamp, including avoiding overheating of the electronic components and hot spots near the user, this article studies the development of a predictive heat dissipation model of a head lamp with COMSOL Multiphysics®.

2 Experimental Set Up

The predictive performances of the model will be assessed by comparing its results with experimental data obtained in laboratory on an existing device.

The existing head lamp, illustrated in Figure 1, is composed of electronic components (magenta), sources of heat, brazed on a PCBA (green and copper red) dissipating and distributing part of the heat towards the rest of the lamp, mounted on a polycarbonate (PC) structure (blue), fixed by steel screws to a PC enveloping shell (gray), closing the lamp. The lamp also contains a battery (deep blue), a lens (yellow) fixed to the enveloping shell, and an aluminum dissipator (not shown) on the back of the PCBA behind the LED.

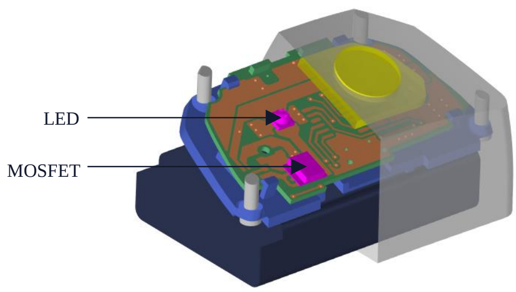

Figure 1. Existing head lamp components. The enveloping shell and the lens (transparent gray) are cropped.

The laboratory is maintained at 23.2 °C. Temperature measurements are performed at stationary state on the lamp working in a continuous light mode. Experimental data are gathered in two configurations.

In case (1), the lamp is *open*, meaning that the enveloping shell, the lens and the screws are removed, and the battery is let far away from the device on the lab bench. The LED targets the laboratory ceil. In this case, the temperature field at the surface of the electronic components and the PCBA is captured using a thermal camera.

In case (2), the lamp is *closed* and equipped with thermocouples, positioned on the cases of the LED and the MOSFET, but also on the aluminum dissipator, bringing local temperature data in normal operating conditions. The LED targets the laboratory walls: the lamp is in its operating orientation.

3 Numerical Model

a. Conduction and Nat. Convection: Open Case

The first version of the model seeks to reproduce the experimental results of case (1), by taking into account heat transfers by conduction and natural convection. The model is built upon a realistic 3D geometry of components of the head lamp (Figure 1).

Prior setting up the model, the Grashof number has been estimated to assess *a priori* the flow regime in natural convection:

$$G_r = \frac{g \cdot |\beta_0| \cdot \Delta T \cdot \rho_0^2 \cdot L^3}{\mu_0^2} \approx 10^7 \ll 10^9, \qquad (1)$$

where g is the gravitational acceleration ($9.81\ \mathrm{m^2/s}$), β_0 is the dilatation coefficient of air ($-3.4 \cdot 10^{-3}\ 1/\mathrm{K}$), ΔT is the order of magnitude of temperature differences (90 K), ρ_0 is the air density ($1.2\ \mathrm{kg/m^3}$), μ_0 is the air dynamic viscosity ($1.8 \cdot 10^{-5}\ \mathrm{Pa \cdot s}$), and L is a characteristic length ($\approx 10\ \mathrm{cm}$). β_0, ρ_0 and μ_0 are given at ambient temperature and atmospheric pressure. As $G_r \ll 10^9$, the natural convection flow is laminar [1].

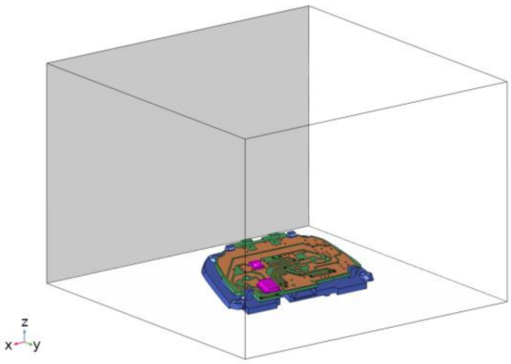

Figure 2. Geometry in the open case, composed of the open lamp, and the surrounding air.

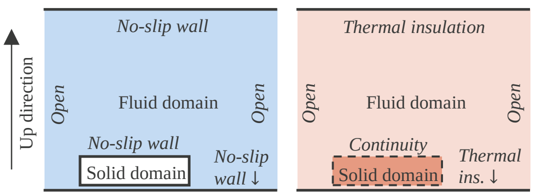

(a) CFD *(b) Heat transfer*

Figure 3. Schematic representation of the conduction-natural convection model of the open lamp.

The computational domain is illustrated in Figure 2, and is composed of *solids* composing the lamp (in color) and a *fluid* – air – (in white). The air flow and the heat dissipation are computed at steady-state. The electronic components produce heat by Joule effect, and each one is modelled as an *Isothermal Domain* and a volumetric *Heat Source*. In the model, the temperature of each electronic component is then an average temperature of the whole component. The produced heat is dissipated in solids and air.

In air (Figure 3.a), compressible Navier-Stokes equations and Heat Transfer in Fluids are solved:

$$\nabla \cdot (\rho \boldsymbol{u}) = 0, \qquad (2)$$

$$\begin{gathered} \rho \boldsymbol{u} \cdot \nabla \boldsymbol{u} = \nabla \cdot (-p\mathbf{I} + \mathbf{K}) + \rho \boldsymbol{g}, \\ \mathbf{K} = \mu[\nabla \boldsymbol{u} + (\nabla \boldsymbol{u})^{\mathrm{T}}], \end{gathered} \qquad (3)$$

$$\rho c_p \boldsymbol{u} \cdot \nabla T - \nabla \cdot (k \nabla T) = Q, \qquad (4)$$

$$\begin{gathered} \rho = \rho(p, T), \\ \mu = \mu(T), \\ c_p = c_p(T), \\ k = k(T), \end{gathered} \qquad (5)$$

where $\boldsymbol{u}$ (m/s) is the air velocity, p (Pa) the absolute pressure, T (K) is the temperature, ρ ($\mathrm{kg/m^3}$) the air density, μ (Pa · s) the air dynamic viscosity, $\boldsymbol{g}$ ($\mathrm{m/s^2}$) the gravity vector, c_p (J/kg · K) the air heat capacity, k (W/m/K) the air thermal conductivity, and Q ($\mathrm{J/m^3}$) is the sum of heat sources. ρ, μ and c_p are given by the *built-in Air material*.

The heat transfer in solids (Figure 3.b) are modelled by the steady-state heat equation:

$$-\nabla \cdot (k \nabla T) = Q, \qquad (6)$$

where k is the solid thermal conductivity, depending on the nature of each material. Copper pads on the PCBA (Figure 1 – copper red) are very thin compared to the rest of the geometry, and are modelled using shells, assuming that the temperature gradient within the thickness is negligible. The heat transfers in these shells are characterized by the shell thickness e (m) and its thermal conductivity k.

The boundary conditions are illustrated in Figure 3. In CFD, open boundaries put a constraint on the pressure, while the no-slip walls induce head losses, which puts a constraint on the velocity, and closes the equations. In heat transfer, air at ambient temperature (laboratory temperature) is brought by incoming flows using the open boundaries condition. Temperature and heat fluxes are continuous at the solids/fluid interface.

These equations are implemented in COMSOL using the Nonisothermal Laminar Flow interface with Thin Layers using the thermally thin approximation [2].

b. Adding Radiative Transfers: Closed Case

The second version of the model seeks to reproduce the experimental results of case (2). For more accuracy, the radiation is taken into account.

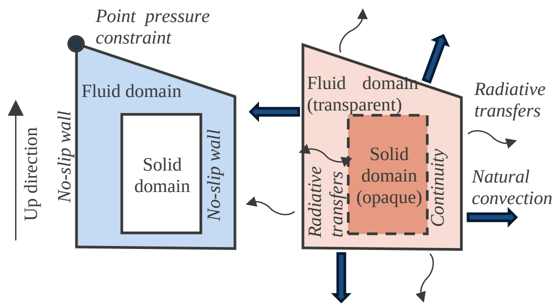

(a) CFD *(b) Heat transfers*

Figure 4. Schematic representation of the conduction-natural convection-radiation model of the closed lamp.

The computational domain is the closed lamp (Figure 1), and the model features are schematized in Figure 4. The air surrounding the lamp is not modelled explicitly.

Within the lamp, Eq. 2-6 describe heat transfer by conduction (solids) and natural convection (fluid) in the lamp. The heat transfer within the enveloping shell (Figure 1 – gray) is modelled using thermally thin shells. The Navier-Stokes equations are closed using no-slip boundary conditions on all the boundaries of the fluid domain and a point pressure constraint (Figure 4.a).

Heat transfer by radiation inside the lamp is taken into account using a diffuse gray bodies surface-to-surface radiation model. Each solid surface is characterized by its emissivity ε (1), emitting heat by radiation according to the Stefan-Boltzmann equation:

$$q_{emittance} = \varepsilon\, \sigma\, T^4, \tag{7}$$

where σ $(\mathrm{W/m^2/K^4})$ is the Stefan-Boltzmann constant. The heat emitted from a solid surface travels through air (refraction index $n = 1$) and is either absorbed or reflected by another solid surface. Absorptivity α and diffuse reflexivity ρ_d are obtained as follows:

$$\begin{aligned} \alpha &= \varepsilon, \\ \rho_d &= 1 - \varepsilon. \end{aligned} \tag{8}$$

The radiosity J, the amount of radiation leaving each point of solid surfaces, is obtained by summing emittance and diffuse reflectance:

$$J = q_{emittance} + \rho_d\, G, \tag{9}$$

where G is the irradiance, the amount of incident radiation, function of the radiosity on all surfaces and view factors. A boundary source term is added to include the effect of radiation to the heat balance, expressed as the difference of absorbed radiation with emittance:

$$\boldsymbol{q_{rad}} \cdot \boldsymbol{n_{fluid,int}} = \alpha\, G - q_{emittance}, \tag{10}$$

where $\boldsymbol{n_{fluid,int}}$ is the interior normal of the fluid domain.

Heat finally dissipates into the environment by natural convection and radiation, modelled as follows:

$$\boldsymbol{q} \cdot \boldsymbol{n} = h(T - T_{ext}) + \varepsilon\, \sigma\, (T - T_{ext})^4, \tag{11}$$

where h is the natural convection heat transfer coefficient. A prior analysis gives $h = 10\ \mathrm{W/m^2/K}$.

The surface-to-surface radiative heat transfers are implemented in COMSOL using the Surface-to-Surface Radiation physics with Diffuse Surfaces. The heat exchanges with the environment are implemented using Heat Flux boundary conditions with appropriate heat transfer coefficients.

c. Numerical Aspects

Eq. 3 is numerically implemented in the “reduced pressure” form [3], in order to maximize the accuracy of pressure fluctuations being far less than atmospheric pressure.

A particular attention has been paid to the mesh, *a priori* requiring thin elements near walls to accurately capture heat transfers in the boundary layers, while surface-to-surface heat transfers densify the matrices, requiring limiting the size of the mesh. The Reynolds number is in fact rather low $(10^1 - 10^2)$, and a tetrahedral mesh refined near heat sources and geometrical details (*e.g.* copper pads) has been selected. All the variables ($\boldsymbol{u}$, p, T, and J) are solved using $P1$ elements. Eq. 3-4 are solved using streamline and crosswind stabilization. This discretization results in $1.2\ \mathrm{M}$ degrees of freedom to solve.

The view factors of the surface-to-surface radiative heat transfers are computed using the Hemicube algorithm at resolution 256.

The stationary state is solved with a pseudo time-stepping solver. The nonlinear iterations are solved using a fully coupled constant Newton solver. Variables are carefully scaled. Performing one simulation takes less than $1\ \mathrm{h}$ using $45\ \mathrm{GB}$ of RAM on 8 cores of a recent laptop.

4 Results and Discussion

a. Case (1) - Open Case

In case (1), the temperature field on the PCBA is captured thanks to a thermal camera, allowing to locate hot spots and observe temperature gradients, as shown in Figure 5. Copper pads are recognizable as contiguous areas having a near homogeneous temperature.

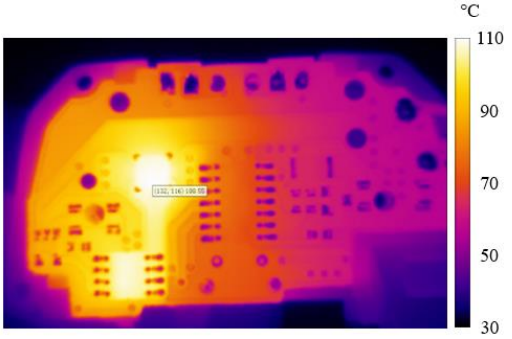

Figure 5. Experimental open case surface temperature field captured by a thermal camera. The hot spots are located on the LED and the MOSFET.

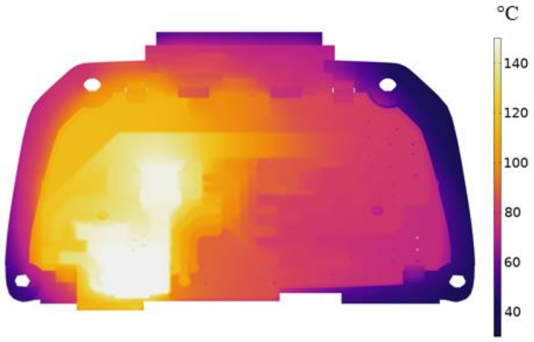

Figure 6. Numerical open case temperature field obtained using the model described in section 3.a.

Using the model described in section 3.a, it is possible to represent the temperature field on the PCBA with the same point of view, as shown in Figure 6.

Qualitatively, numerical results are consistent with experimental ones, locating at the same place hot spots, reproducing comparable global temperature gradients, and predicting near homogeneous temperatures on the copper pads.

Quantitatively, the predicted temperature is globally too high compared to experimental measurements (*e.g.* model LED temperature: 150 °C vs. experimental LED temperature: 110 °C), and more accuracy is needed. A deep verification of materials and components specification has been performed in order to remove any doubts on the model input data. So far, radiative heat transfers have been neglected, and may explain and reduce the model-experience temperature gap.

b. Case (2) - Closed Case

In case (2), the temperature is measured at specific locations using thermocouples. Numerically, the model described in section 3.b is used to evaluate local temperature at the same locations. Two variations of the model are compared to evaluate the impact of radiation: with and without radiative heat transfers. Numerical and experimental results are summarized in Table 1.

Table 1. Numerical and experimental local temperature results.

Location	Model (°C)		Exp (°C)
	w/o rad.	w/ rad.	
LED	152	114	120
MOSFET	158	126	124
Al dissipator	134	105	99

The model neglecting radiative heat transfers is poorly accurate, overestimating the local temperatures of 30 K – 35 K. These differences are too high, making it difficult to know if the electronic components are below the maximal admitted temperature. The model including radiation is far more accurate, having a difference of less than 6 K to experimental results. These results show that the radiation seems to be of prime importance in the heat dissipation capacities of the lamp. This model, including all the heat transfer modes, can be retained to serve as a design support tool.

5 Conclusions

The goal of this work is to build a predictive numerical model for the heat dissipation of a head lamp. The model starts from a realistic 3D geometry of an existing device, and is built in two stages, first taking into account conduction and natural convection, and second adding the radiative heat transfers.

The surface temperature of the PCBA predicted by the conduction-natural convection model have been compared to experimental data obtained on the open lamp using a thermal camera, showing a good qualitative agreement, but high quantitative differences (≈ 40 K). When the lamp is closed, experimental local temperature measurements are available thanks to thermocouples. The effect of enabling of not the radiative transfers have been quantified, showing that modelling radiation was of prime importance, reducing the model temperature biases from ≈ 30 K to ≈ 5 K, validating the modelling approach.

The model can then be used to evaluate the effects on the thermal dissipation performance of employing new materials and shapes to evolve parts of the lamp.

References

[1] A. Bejan, in *Convection Heat Transfer*, 3 ed., John Wiley & Sons, 2004, p. 215.

[2] COMSOL, "Thin Layer - Thermally Thin Approximation," in *Heat Transfer Module User's Guide*, 2021, pp. 225-227.

[3] COMSOL, CFD Module User's Guide, 2021.

Acknowledgements

This work has been founded by DECATHLON and made in a fruitful collaboration between DECATHLON and SIMTEC.